99-1

Ochs M.

E1-99-1

TRANSMUTATION OF ^{129}I AND ^{237}Np USING SPALLATION NEUTRONS PRODUCED BY 1.5, 3.7 AND 7.4 GeV PROTONS

1999

Образцы двух долгоживущих радиоактивных нуклидов — йода-129 и нептуния-237
— с массой порядка 1 г помещались в поле электроядерных нейтронов, которые
образуются в небольших металлических мишенях из свинца и урана, бомбардируемых
протонами и окруженных слоем парафинового замедлителя толщиной 6 см. Одновре-
менно с этим обычные активационные детекторы из хлорида лантана и окиси урана
и различные твердотельные ядерные трековые детекторы (SSNTD) экспонировались
в потоках вторичных нейтронов в ходе этих экспериментов, выполненных на пучках
синхрофазотрона Лаборатории высоких энергий ОИЯИ (Дубна) при энергиях протонов
1,5, 3,7 и 7,4 ГэВ. Для двух указанных радиоактивных нуклидов определена скорость их
трансмутации в (n,γ)-реакции. Значения наблюдаемых потоков вторичных нейтронов
оказываются систематически большими по сравнению с вычисленными по известным
моделям LAHET (Лос-Аламос) и DCM-CEM (Дубна).

Small samples of approximately 1 g of ^{129}I and ^{237}Np, two long-lived radioactive waste
nuclides, were exposed to spallation neutron fluences from relatively small metal targets
of lead or uranium, surrounded with a paraffin moderator 6 cm thick irradiated with 1.5, 3.7
and 7.4 GeV protons. The (n,γ) transmutation rates have been determined for the two
radioactive waste nuclides. Conventional radiochemical La and U sensors and a variety
of solid-state nuclear track detectors were irradiated simultaneously with secondary neutrons.
The observed secondary neutron fluences appear to be systematically larger, as compared
to the calculations with the well-known cascade codes (LAHET from Los Alamos and DCM-
CEM from Dubna).

M.Ochs, J.-S.Wan[1], Th.Schmidt, E.-J.Langrock, P.Vater, R.Brandt[2]

Institut für Physikalische, Kern- und Makromolekulare Chemie, FB 15, Philipps-Universität, Marburg, Germany

J.Adam[3], V.P.Bamblevski, V.Bradnova, L.Gelovani[4], T.G.Gridnev, V.G.Kalinnikov, M.I.Krivopustov, B.A.Kulakov, A.N.Sosnin, V.P.Perelygin, V.S.Pronskikh, V.I.Stegailov, V.M.Tsoupko-Sitnikov

Joint Institute for Nuclear Research, Dubna

G.Modolo, R.Odoj, P.-W.Phlippen

Forschungszentrum Jülich, Jülich, Germany

M.Zamani-Valassiadou

Physics Department, Aristotle University, Thessaloniki, Greece

J.C.Adloff, M.Debeauvais

Institute de Recherche Subatomique, Strasbourg, France

S.R.Hashemi-Nezhad

Department of High Energy Physics, School of Physics, University of Sydney, Sydney, Australia

S.-L.Guo, L.Li, Y.-L.Wang

China Institute of Atomic Energy, Beijing 102413, China

K.K.Dwivedi

Department of Chemistry, North-Eastern Hill University, Shillong, India

I.V.Zhuk, S.F.Boulyga, E.M.Lomonossova, A.F.Kievitskaja, I.L.Rakhno, S.E.Chigrinov

Institute of Power Engineering Problems, Minsk, Belarus

B.Wilson

Los Alamos National Laboratory, Los Alamos, NM, USA

[1]Permanent address: Northwest Institute of Nuclear Technology, Xian, China
[2]Corresponding author, e-mail: brandtr@mailer.uni-marburg.de
[3]Permanent address: Nuclear Physics Institute, Rez, Czech Republic
[4]Permanent address: Institute of Physics, Georgian Academy of Sciences, Tbilissi, Georgia

1. Introduction

A rather new and fundamental nuclear technology has begun to occupy the scientific discussion in the last decade. Due to progress in the economic construction of high-intensity, high-energy accelerators, say 1 GeV proton accelerators of about 1 mA or even higher intensities, one could think about social-industrial applications. Some aspects of these problems could be summarrized as follows:

1.Economical and safe production of electricity in subcritical nuclear power plants, called energy amplifiers, as suggested, for instance, by Tolstov [1] and by Rubbia and coworkers [2]. Such machines would have certain advantages in the construction and operation (no risk of Tchernobyl type). However, they are not free of technical risks. When operated with thorium as nuclear fuel, they avoid the production of transuranium problem nuclides, in particular plutonium.

2.The use of the same technology to transmute long-lived radioactive waste nuclei, such as ^{129}I, ^{99}Tc and the minor actinides (^{237}Np, Am, Cm isotopes), into short-lived fission products, as suggested by scientists from the Los Alamos National Laboratory (e.g. Ref. [3]). In this way the problem of nuclear waste storage could be solved. One would need only final depositories which must be kept separated from the biosphere for about 600 years instead of millions of years.

3.This new technology obviously has also some aspects which need careful monitoring - for example by the IAEA (Vienna) so that the available techniques are not misused for the production of materials which require the strictest surveillance due to international treaties [4-7].

Up to now, there has been an abundance of theoretical publications on various aspects of NWT (Nuclear Waste Transmutation). However, the empirical situation has been studied to a much lesser extent. To our knowledge, there exist only two communications on the experimental transmutation of ^{129}I and ^{237}Np using relativistic particle beams [8, 9]. These two nuclides are problem nuclides of radioactive waste due to their very long half-lives (> 10^5 yr). In this paper we extend these studies of the transmutation of ^{129}I and ^{237}Np using 1.5, 3.7 and 7.4 GeV protons.

As the direct transmutation rates are obviously the result of our specific experimental arrangements, we have tried to generalize our results to some extent. For this reason, we studied the number of secondary neutrons produced in our setup, using a variety of radiochemical and solid state nuclear track detectors (SSNTD) techniques. The results were compared to theoretical model calculations such as those using the LAHET (Los Alamos) and the DCM-CEM (Dubna).
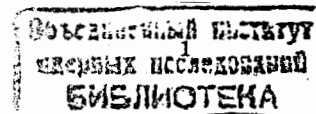
Furthermore a comparison was made with the results from [10]. Finally, we present the results in terms of conventional (n,γ)-cross-sections for the transmutation of ^{129}I and ^{237}Np under our experimental conditions.

2. Experimental

The experiments were carried out at the Synchrophasotron, Laboratory for High Energies (LHE), Joint Institute for Nuclear Research (JINR), Dubna in Russia. Some details of the irradiation are given in Tables 1 and 2. The different experiments will be described consecutively.

During the 1997 experiment, we had some problems in determining the proton fluences at energies 1.5 and 7.4 GeV, as we employed the radiochemical sensor Al → ^{24}Na in close contact to the thick metal target. As is known from [11] and our own unpublished work, one obtains significantly incorrect results under these conditions due to ^{27}Al$(n,\alpha)^{24}$Na reactions. We carried out another experiment at 1.5 GeV in 1998 and determined with two independent radiochemical sensors that this time the operators gave correct proton fluences within ±10% (to be published). In addition, we determined the fluence in the 1.5 GeV p + U (Pb) irradiation with an U → ^{24}Na sensor, confirming the values given by the operators.

Table 1. Experiments with ^{129}I and ^{237}Np using Pb and U targets as a neutron spallation source (3.7 GeV p in 1996; 1.5 GeV p and 7.4 GeV p in 1997)

Experiment	Beam time	Fluence[1, 2]	Radiochemical sensor
1.5 GeV p + Pb	1.17 h	$1.40 \cdot 10^{13}$ (±20%)	
1.5 GeV p + U	2.14 h	$1.50 \cdot 10^{13}$ (±20%)	U → ^{24}Na (1)
3.7 GeV p + Pb	0.15 h	$1.24 \cdot 10^{13}$ (±15%)	Cu → ^{24}Na (1)
3.7 GeV p + U	0.27 h	$1.24 \cdot 10^{13}$ (±15%)	Cu → ^{24}Na (1)
7.4 GeV p + Pb	1.36 h	$0.90 \cdot 10^{13}$ (±20%)	
7.4 GeV p + U	3.35 h	$0.90 \cdot 10^{13}$ (±20%)	U → ^{24}Na (2)

(1) Agrees within ±10% with the data provided by the accelerator operators. Both 1.5 GeV irradiations had been given about the same fluence by the operators.

(2) The Dubna operators gave at 7.4 GeV for both targets a fluence of $(1.6\pm0.1) \cdot 10^{13}$. The sensor U → ^{24}Na gave a fluence of $0.9 \cdot 10^{13}$ using a cross-section of 14.1 mb. This latter was chosen by us for measurements as the proper half-life (15.0 h) of the ^{24}Na-gamma line 1368.5 keV.

Table 2. Experiment with ^{129}I and ^{237}Np directly exposed to a 3.7 GeV proton beam (1996)

Experiment	Beam time	Fluence[1]
3.7 GeV p + ^{129}I / ^{237}Np	0.25 h	$1.25 \cdot 10^{13}$ (±15%)

(1) Measured radiochemically with the sensor Cu → ^{24}Na. Does not differ significantly from the value obtained by accelerator operators.

2.1. Transmutation experiments on ^{129}I and ^{237}Np

The Pb target (Fig. 1), a cylinder of 20 cm Pb, composed of 20 disks, each 8 cm in diameter and 1 cm thick, was irradiated with a well-focused beam of 1.5, 3.7 and 7.4 GeV protons. The fluence was about 10^{13} protons. The full width at half-maximum of the beam was about 22 mm as measured with SSNTD in front of the first Pb disk (see Ref. [6] and later in this paper, section 2.4.6).

The Pb cylinder was surrounded by a paraffin moderator 6 cm thick. Transmutation studies were also carried out using a similar U target (Fig. 2) in order to investigate the influence of the Z of the metallic target and the amount of secondary neutrons produced. Details are given in the next section.

The samples of 0.5 g iodine with 15% ^{127}I and 85% ^{129}I (in form of NaI) and 0.742 g ^{237}Np (in form of NpO$_2$) were placed on top of the moderator. The isotopic composition of this iodine target is typical for the iodine radioactive wastes from a nuclear power plant. The iodine isotopes were obtained from the Bochvar Institute in Moscow (VNIINM). The radioactive samples of I and Np were well-sealed in Al capsules (Fig. 3). They were prepared by the Institute of Physics and Power Engineering (Obninsk, Russia).

Furthermore, two other samples, ^{129}I and ^{237}Np, were irradiated directly in the 3.7 GeV proton beam with $1.25 \cdot 10^{13}$ protons during a separate irradiation (Fig. 4). After the irradiation, the radioactive samples were placed in front of a HPGe detector to measure the gamma activity. As both ^{129}I and ^{237}Np samples are fairly radioactive even without any activation, they were placed at a distance of 20 cm from the detector. For the ^{237}Np sample, a Pb plate 1 cm thick was placed between the sample and the detector, reducing considerably the low energy activity. We identified in the lead and uranium targets (Figs. 1 and 2) the (n,γ)-reaction products ^{130}I and ^{238}Np (Figs. 5 and 6). The decay curves for these two nuclides have already been published [8, 9]. In addition we could identify also a tiny activity due to ^{126}I in the NaI samples as shown in the gamma spectra (Fig. 6). Further analysis of the gamma spectra by state-of-the-art techniques
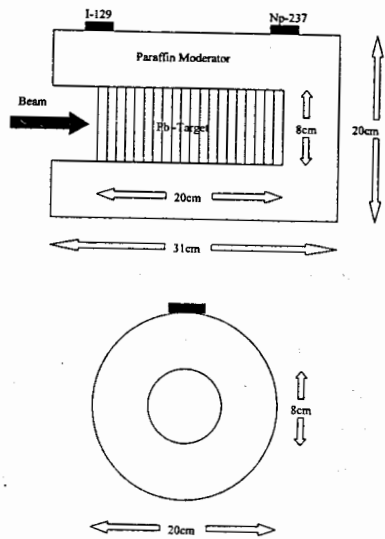
Fig. 1. ^{129}I and ^{237}Np samples on top of the Pb target (1.5, 3.7 and 7.4 GeV protons), side view and top view
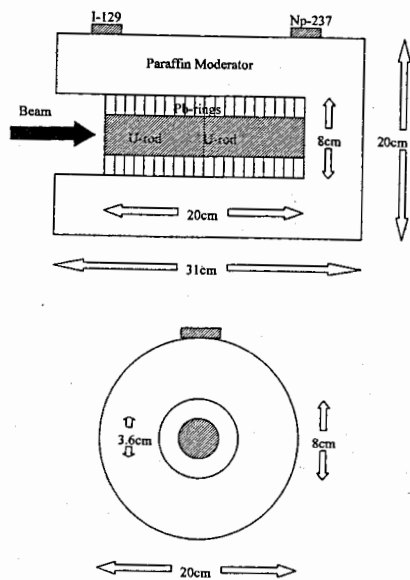

Fig. 2. ^{129}I and ^{237}Np samples on top of the U target (1.5 and 7.4 GeV protons), side and top view
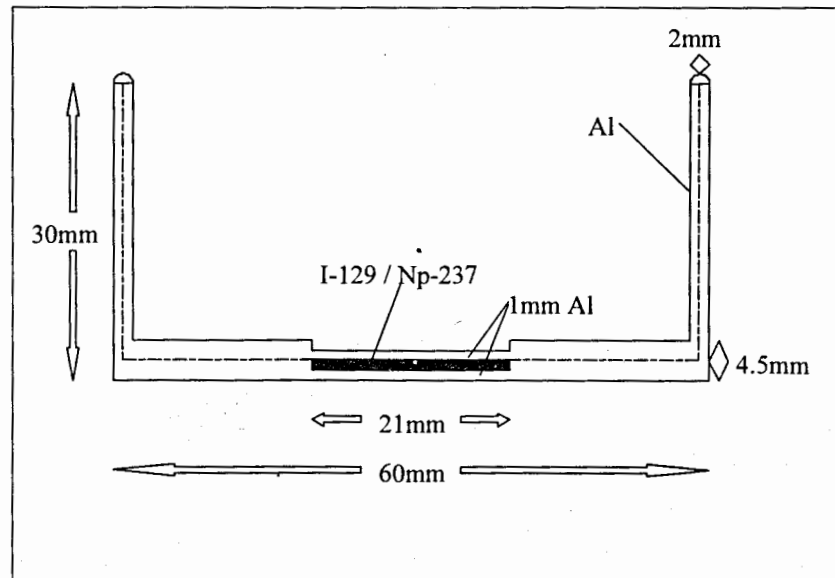

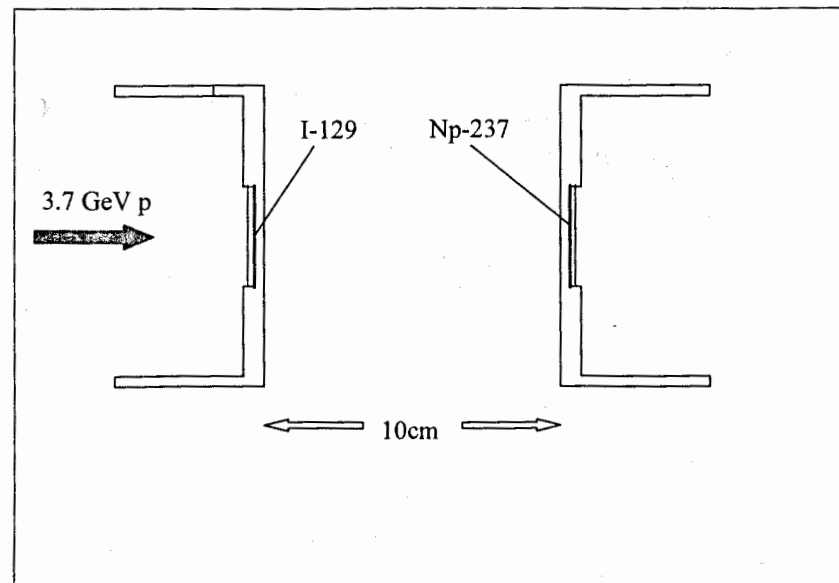Fig. 3. ^{129}I and ^{237}Np samples in Al container

Fig. 4. Setup for the direct irradition of ^{129}I and ^{237}Np with 3.7 GeV protons
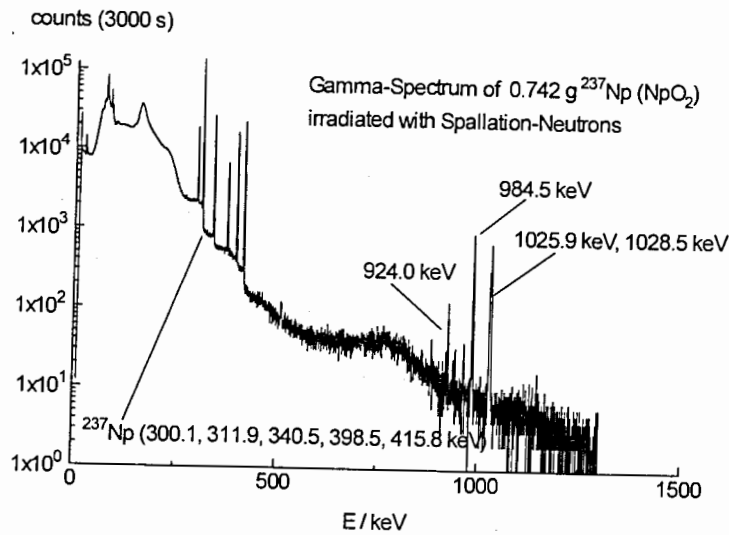
Fig. 5. Spectrum of ^{237}Np irradiated with spallation neutrons from an U target (7.4 GeV p) hielded with 1cm Pb: ^{238}Np (924, 984, 1026, 1028 keV)
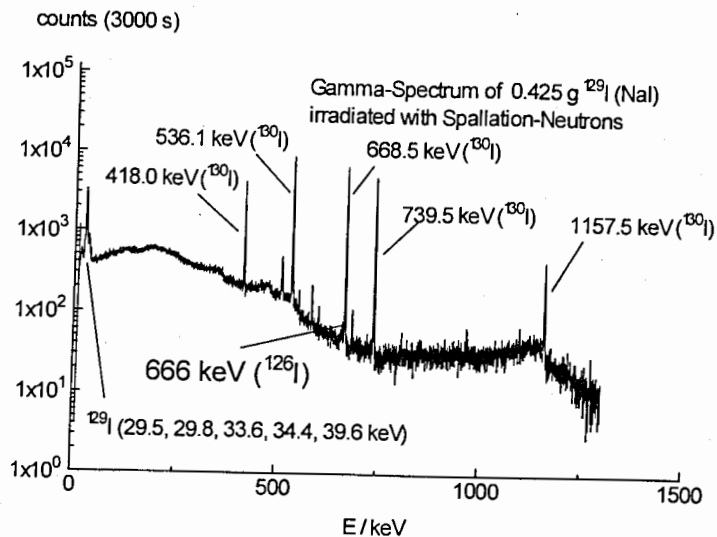

Fig. 6. Spectrum of ^{129}I irradiated with spallation-neutrons from an U target (7.4 GeV p): ^{130}I (418, 536, 668, 739, 1157 keV)

is described in references [5-8]. The results are expressed in terms of breeding rates $B_{exp}(A^Z)$ for the production of the nuclide (A^Z) defined as follows:

$$B_{exp}(A^Z) = \frac{\text{number of produced nuclei with} A^z}{(\text{single incident ion}) \cdot (1\text{g target isotope})} \quad (1.a)$$

or formulated in an equivalent manner for proton-experiments:

$$B_{exp}(A^Z) = \frac{\text{total number of produced nuclei with} A^z}{(\text{proton fluence}) \cdot (1\text{g target isotope})} \quad (1.b)$$

$B_{exp}(A^Z)$ is defined strictly in an empirical manner: It means that ^{129}I is placed at the geometrical position given in Figs. 1 and 2. These target systems were irradiated with relativistic protons. The resulting B_{exp} values are shown later.

In the direct irradiation of ^{129}I and ^{237}Np (Fig. 4) one could observe a large variety of spallation products for ^{129}I as well as some fission products of ^{237}Np, as shown in Figs. 7 and 8. The experimental results are compared with the results obtained with the semi-empirical formula of Rudstam and others [12-14]. This pattern of observed cross-sections for spallation products of Iodine as a function of the mass of the spallation product fits well into the known spallation product behaviour, as described also by Modolo [15].

2.2. Transmutation experiments on depleted uranium and lanthanum

The ^{129}I and ^{237}Np samples have been irradiated under specific geometric conditions as described above. In order to obtain a more general picture of what is going on physically within the target system, it appears useful to study the fluences of secondary neutrons within these target systems themselves. For practical purposes, it is impossible to measure neutrons with their wide range of energies, from thermal up to GeV energies, within the relatively small target systems using standard electronic neutron counters. We had to use a considerably simpler experimental apparatus, i.e. radiochemical and SSNTD sensors. This technique has been used earlier [4-9]. Although our rather simple experimental technique cannot give very detailed and precise results, it could be shown that it gives useful results. The preceding paper [9] described in detail how one obtained neutron fluences with a large variety of sensors in the Pb target (Fig. 1) irradiated with 3.7 GeV protons. In this paper, we want to present a more generalized method of obtaining neutron fluences in both targets used at all the three proton energies employed. For this we have to describe beforehand the experimental determination of the breeding rates B_{exp}.

The target setups for these measurements are shown in Fig. 9. The Pb target has already been described as it was used for ^{129}I and ^{237}Np studies. The uranium target (called U(Pb) target)
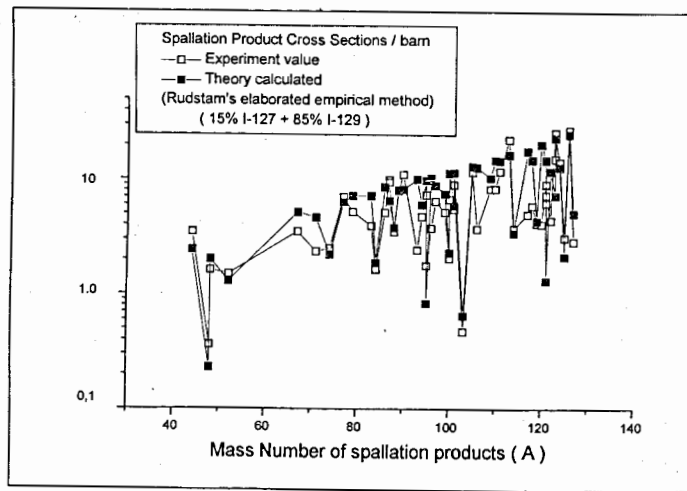
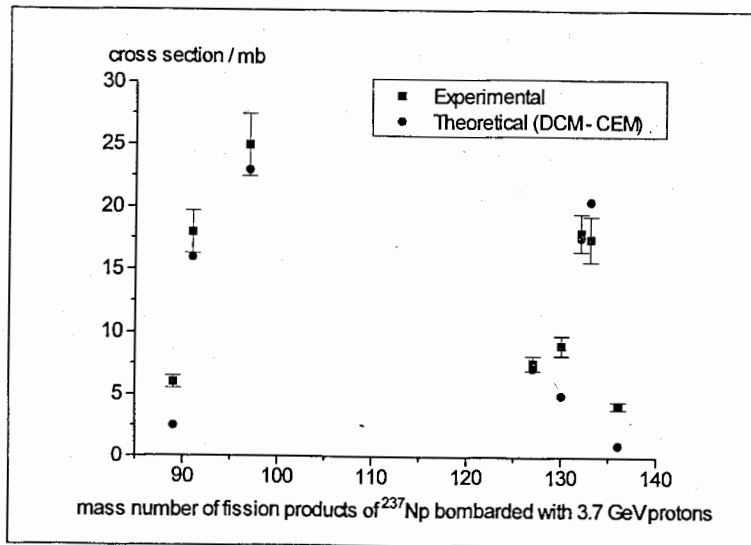Fig. 7. Cross-section for the spallation products of ^{129}I directly irradiated with 3.7 GeV protons

Fig. 8. Cross-section for the fission products of ^{237}Np directly irradiated with 3.7 GeV protons

is shown in Fig. 2. It contained two rods of natural uranium, 3.6 cm in diameter and 10.4 cm long encapsulated in thin Al foils and placed in the centre of a lead target 8 cm in diameter and surrounded again by a paraffin moderator 6 cm thick. Both target systems (Figs. 1, 2 and 9) contained small La sensors as well as small U sensors on their surface. The La and U sensors are shown in Fig. 9. Using the La sensors (1g La in LaCl$_3$ ·(7 H$_2$O)) one could study the neutron fluence via the reaction:

$$^{139}La(n,\gamma)^{140}La \xrightarrow[T_{1/2}=40\ h]{\beta^-} {}^{140}Ce\,. \qquad (2)$$
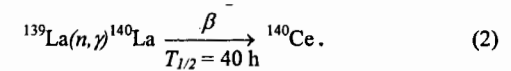
Using the U sensors (1g depleted uranium in UO$_2$·(H$_2$O) with 0.42% ^{235}U) one could study the neutron fluence via the reaction:

$$^{238}U(n,\gamma)^{239}U \xrightarrow[T_{1/2}=24\ min]{\beta^-} {}^{239}Np \xrightarrow[T_{1/2}=2.3\ days]{\beta^-} {}^{239}Pu\,. \quad (3)$$
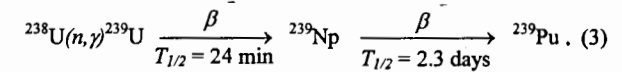
After irradiation, the sensors were analyzed for their gamma activity. The results were registered in the form of B_{exp} values, $B_{exp}(^{140}La)$ and $B_{exp}(^{239}Np)$, on the surface of the moderator. The azimuthally arranged La sensors, spaced equally (60°) in the middle and on the surface of the moderator, allowed the correction for the azimuthal variation of secondary neutrons due to the non-circular beam distribution of the incident proton flux within a plane perpendicular to the beam direction. Using these results, one could calculate average B_{exp} values for ^{140}La and ^{239}Np on the outer mantle of the paraffin moderator for all six target systems under study, as shown in Table 3. The average B_{exp} values for samples 1 - 5 on top of the moderator were corrected for the azimuthal neutron flux distribution. This procedure is described in Refs. [6-9]. The B_{exp} values of the ^{129}I and ^{237}Np sensors are shown in Table 4.

Table 3. Average B_{exp} values for the neutron monitors on the outer surface of the paraffin moderator for Pb and U(Pb) target systems [5-7]

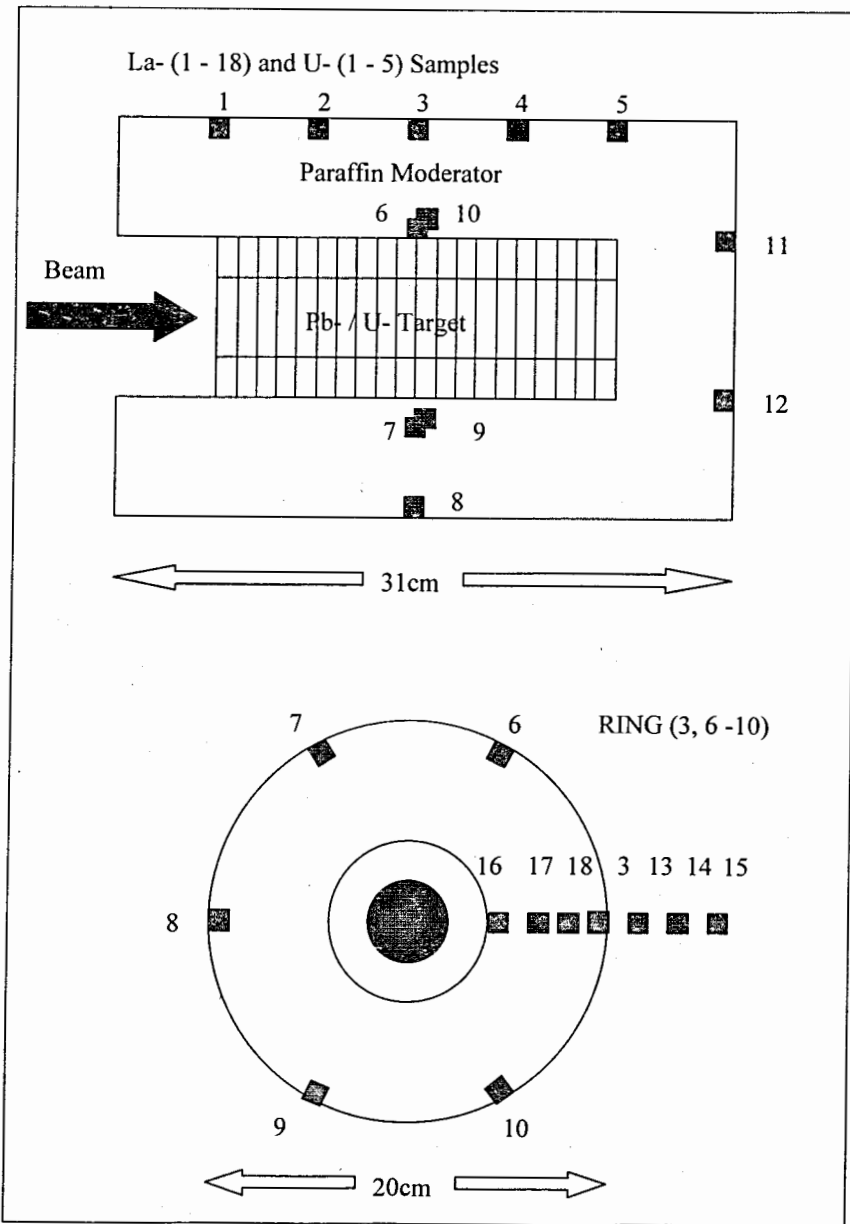| Proton energy	Pb target $B_{exp}(^{140}La)$	Pb target $B_{exp}(^{239}Np)$	U(Pb) target $B_{exp}(^{140}La)$	U(Pb) target $B_{exp}(^{239}Np)$
1.5 GeV	$(1.7 \pm 0.4) \cdot 10^{-4}$	$(0.75 \pm 0.15) \cdot 10^{-4}$	$(3.1 \pm 0.7) \cdot 10^{-4}$	$(1.4 \pm 0.3) \cdot 10^{-4}$
3.7 GeV*	$(6.0 \pm 0.9) \cdot 10^{-4}$	$(2.9 \pm 0.4) \cdot 10^{-4}$	$(10.5 \pm 1.6) \cdot 10^{-4}$	$(4.5 \pm 0.7) \cdot 10^{-4}$
7.4 GeV	$(7.3 \pm 1.5) \cdot 10^{-4}$	$(3.3 \pm 0.7) \cdot 10^{-4}$	$(15.4 \pm 3.1) \cdot 10^{-4}$	$(6.0 \pm 1.2) \cdot 10^{-4}$

* Taken from Ref. [9].

Fig. 9. La and U sensors on the surface of the targets (1.5, 3.7 and 7.4 GeV protons), side view and top view. In positions (1 - 5) La and U sensors are embedded into the moderator within close proximity of approximately 1cm

Table 4. B_{exp} values for the ^{129}I and ^{237}Np samples on the outer surface of the paraffin moderator for Pb and U(Pb) target systems

Proton energy	Pb target B_{exp} (^{130}I)	Pb target B_{exp} (^{238}Np)	U(Pb) target B_{exp} (^{130}I)	U(Pb) target B_{exp} (^{238}Np)
1.5 GeV	$(0.9 \pm 0.2) \cdot 10^{-4}$	$(8.1 \pm 1.6) \cdot 10^{-4}$	$(2.3 \pm 0.5) \cdot 10^{-4}$	$(9.0 \pm 1.8) \cdot 10^{-4}$
3.7 GeV	$(3.1 \pm 0.5) \cdot 10^{-4}$	$(44 \pm 7) \cdot 10^{-4}$	-	-
7.4 GeV	$(4.0 \pm 0.8) \cdot 10^{-4}$	$(41 \pm 9) \cdot 10^{-4}$	$(14.7 \pm 3.0) \cdot 10^{-4}$	$(50 \pm 10) \cdot 10^{-4}$

* Taken from Refs. [8] and [9].

It is interesting to note that all B_{exp} values for ^{140}La and ^{239}Np increase by a factor (3.5 ± 0.5) with increasing proton energy from 1.5 up to 3.7 GeV. This is according to expectations and is well known from other experiments [6-9]. However, we observe only a slight increase in B values when going from 3.7 up to 7.4 GeV. This is against the experimental evidence from other experiments [16]. At present we can give no explanation for this fact. It cannot be excluded that there have been some problems with measuring beam intensities at 7.4 GeV or that our target is too short.

It was shown [9] that the experimental B_{exp} (^{239}Np) value for 3.7 GeV proton induced reactions in the uranium target 10 cm behind the entrance of the beam into U and then 10 cm perpendicular off axis agreed with the corresponding B_{exp} (fission) value from the experiment [10] using 2.7 GeV protons. The experimental results from both laboratories agree, despite some differences in the experimental arrangements. One should remember that it was shown extensively that B_{exp}(^{239}Np) = $(1.0 \pm 0.1) \cdot B_{exp}$(fission) in natural uranium [9].

This reaction pattern is reproduced in this experiment at a proton energy of 1.5 GeV:

$$B_{exp}(^{239}\text{Np}) = (2.2 \pm 0.5) \cdot 10^{-4} \qquad \text{(the given paper)}$$
$$B_{exp}(\text{fission}) = (3.2 \pm 0.5) \cdot 10^{-4} \qquad \text{(ref. [17])}.$$

Additionally, it is an experimental fact that for a given distance of approx. 10 cm off axis from the beam direction and 10 cm behind the entrance of the beam into the extended Pb targets, all the experimental B(^{239}Np) values for small uranium sensors are in close proximity, increasing linearly to a first order approximation only with the total energy of the incoming relativistic ion [18].

2.3 Estimation of the fluence of secondary neutrons in our targets and comparison with model calculations

Now one must consider the conversion of B_{exp} values into secondary neutron fluences. The primary relativistic proton (E_p) induces nuclear interactions. This produces a fluence of secondary neutrons with energies $0 < E_n \leq E_p$ leaving the outer surface of the moderator. The details of all these nuclear interactions, scattering processes etc. are certainly quite complex, but the result is simple: such (n,γ) nuclear reaction products as ^{140}La and ^{239}Np are observed experimentally. There exist high-energy transport codes, such as LAHET (Los Alamos) and DCM-CEM (Dubna), that allow the calculation of the fluence of secondary neutrons $\Phi_n(E)_{theor}$ on the outer surface of the paraffin moderator. These codes are based on intra-nuclear cascades using the Bertini model, followed by the pre-equilibrium model and then by the Rutherford-Cameron-Cook-Ignatyuk model giving level densities. These two models have been used by the collaboration for 3.7 GeV protons earlier [9]. In this paper Figs. 10 and 11 present the calculated $\Phi_n(E)_{theor}$ on the outer mantle of the moderator, as based on the two codes used for the reaction 1.5 GeV p + Pb. Furthermore, the excitation function for the (n,γ) reactions (equations (2) and (3)) are well known; as a matter of record the excitation function for the $^{238}U(n,\gamma)$ reaction is shown in Fig. 12. Now one can calculate a B_{theor} value for all the systems under investigation:

$$B_{theor}(A^z) = N_T \cdot \int_0^{E_p} \Phi_n(E) \cdot \sigma(n,\gamma)(E) \, dE . \qquad (4)$$

$\Phi_n(E)$ is the average energy dependent neutron fluence per cm^2 per proton on the outer surface mantle of the paraffin moderator. The term $\sigma_{(n,\gamma)}(E)$ is the energy dependent (n,γ) neutron capture cross section. N_T is the number of target atoms in 1g of the target isotope per cm^2. One should remember, that the surfaces of our La and U sensors are also about $1cm^2$. The results for all the various B_{theor} are shown in Tables 5 and 6 and compared to the experimental B values, giving a ratio $R(B)$ defined as follows:

$$R(B) = B_{exp} / B_{theor} . \qquad (5)$$

As one can see from Tables 5 and 6, nearly all $R(B)$ values are larger than 1 with a wide spread in R between 0.7 ± 0.2 and 4.1 ± 0.6. This wide spread in $R(B)$ is not surprising, as both our methods, experimentally and theoretically, are known to be quite approximate. However, we confirm the results from a preceding paper [9] that the discrepancy is larger for such sensors as ^{140}La, which register practically only thermal neutrons, as compared to ^{239}Np, which is also produced to a significant degree by epithermal neutrons. In our experiment there is a very hard
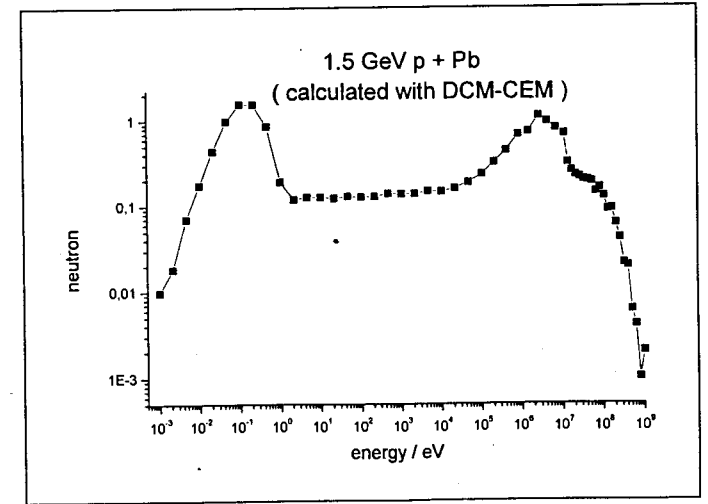

Fig.10. Neutron spectrum for the reaction 1.5 GeV p + Pb, calculated with the DCM - CEM code on the outer mantle of the moderator for one primary proton. Total number of neutrons - 18.6; number of low-energy neutrons ($E < 1$ eV) - 5.9
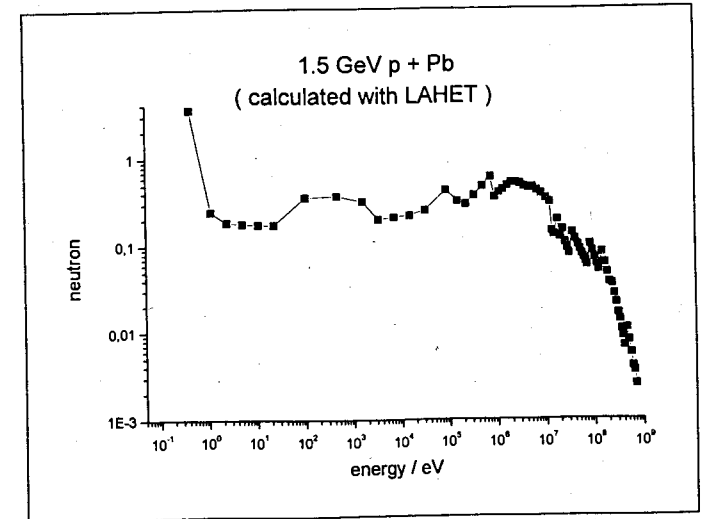

Fig.11. Neutron spectrum for the reaction 1.5 GeV p + Pb, calculated with the LAHET code on the outer mantle of the moderator for one primary proton. Total number of neutrons - 17.5; number of low-energy neutrons (E< 1eV) - 3.8

neutron spectrum, as shown in Figs. 10 and 11. It will be shown later in this paper

that no discrepancy can be observed between experiment and theory when very high

energy neutrons ($E > 30$ MeV) are considered.

Table 5. Theoretical B_{theor} values as based on the DCM-CEM model and the values for
$R(B) = B_{exp}/B_{theor}$

Proton energy	$B_{theor}(^{140}La)$ Pb target	$B_{theor}(^{239}Np)$ Pb target	$B_{theor}(^{140}La)$ U target	$B_{theor}(^{239}Np)$ U target
1.5 GeV	$0.82 \cdot 10^{-4}$ $R(B)=2.1 \pm 0.5$	$0.74 \cdot 10^{-4}$ $R(B)=1.0 \pm 0.2$	$1.84 \cdot 10^{-4}$ $R(B)=1.7 \pm 0.4$	$1.65 \cdot 10^{-4}$ $R(B)=0.8 \pm 0.2$
3.7 GeV	$1.50 \cdot 10^{-4}$ $R(B)=4.0 \pm 0.8$	$1.37 \cdot 10^{-4}$ $R(B)=2.1 \pm 0.4$	$3.56 \cdot 10^{-4}$ $R(B)=2.9 \pm 0.6$	$3.28 \cdot 10^{-4}$ $R(B)=1.3 \pm 0.3$
7.4 GeV	$2.38 \cdot 10^{-4}$ $R(B)=3.1 \pm 0.6$	$1.97 \cdot 10^{-4}$ $R(B)=1.7 \pm 0.4$	$5.71 \cdot 10^{-4}$ $R(B)=2.7 \pm 0.5$	$5.34 \cdot 10^{-4}$ $R(B)=1.2 \pm 0.3$

Table 6. Theoretical B_{theor} values as based on the LAHET model and comparison with
$R(B) = B_{exp} / B_{theor}$

Proton energy	$B_{theor}(^{140}La)$ Pb target	$B_{theor}(^{239}Np)$ Pb target
1.5 GeV	$0.78 \cdot 10^{-4}$ $R(B)=2.2 \pm 0.5$	$1.02 \cdot 10^{-4}$ $R(B)=0.7 \pm 0.2$
3.7 GeV	$1.45 \cdot 10^{-4}$ $R(B)=4.1 \pm 0.6$	$1.87 \cdot 10^{-4}$ $R(B)=1.6 \pm 0.3$

We encountered rather similar problems when investigating the results from [9, 10]. It must be repeated: the experimental results for transmutation in uranium agree for the specified geometrical position at both laboratories at 1.5 GeV and 3.2 ± 0.5 GeV proton energy. However, we are unable to understand both experimental results on the basis of model calculations available to us [9].

Consequently, we think that these effects may be due to one of the following reasons:

1. The theoretical codes underestimate the number of neutrons emitted during the primary interactions of the relativistic proton with the target or do not take into account correctly the properties of the moderator. However, the LAHET code describes the number of secondary

neutrons quite accurately when this number is measured with conventional electronic neutron counters within a moderator medium at some 20-40 cm distance from the beam axis [19].

2. The theoretical codes give the correct number of secondary neutrons, but these neutrons show enhanced nuclear cross sections within about the first 15 cm of interaction path [7-9, 18]. Such an option is not well accepted within the physics community. However, we have no longer any problem of understanding the enhanced "energy amplification" as observed by Andrianmonje et al. [10] and interpreted by Wan et al. [9]. A similar enhanced nuclear cross section has again been observed quite recently by Jain et al. [20], when they investigated heavy secondary fragments produced in nuclear emulsions during an irradiation with 10·A GeV ^{197}Au. This entire field has also been described elsewhere [18].

Our experimental techniques do not allow deciding which option is correct. Consequently, we consider from now on that the number of secondary neutrons is larger than calculated in order to give some quantitative interpretation to our experimental findings. All excesses of experimental results above theoretical estimations will be considered as being due to larger numbers of secondary neutrons than those estimated theoretically. Therefore, we have to estimate the experimental neutron numbers and compare them to theoretical values.

In this estimation of neutron fluences on the outer surface of the paraffin moderator (at $r = 10$ cm) the procedure developed by Wan et al. [9] is used. The total experimental fluence of neutrons $\Phi_n (E)_{exp}$ can be estimated as follows from the experimentally observed B values:

$$\Phi_n(E)_{exp} = \frac{B_{exp} \cdot O_s}{N_T \cdot \sigma_{eff}(n,\gamma)} \quad \text{(per incident proton)} . \quad (6)$$

The B_{exp} values are given in Tables 3 and 4, O_s is the moderator mantle surface (2000 cm^2), N_T the number of target atoms in 1 g of the target per cm^2; $\sigma_{eff}(n,\gamma)$ is the effective (n,γ) cross section for the neutron energy region in which $\Phi_n(E)_{exp}$ will be determined. It can be calculated as follows:

$$\sigma_{eff}(n,\gamma) = \frac{\int_{E_2}^{E_1} \Phi_n(E) \cdot \sigma(n,\gamma)(E) dE}{\int_{E_1}^{E_2} \Phi_n(E) \, dE} . \quad (7)$$

The theoretical neutron fluences $\Phi_n(E)_{theor}$ are given in Figs. 10 and 11 (LAHET- and DCM-CEM code), and an example of a corresponding excitation function is given in Fig. 12. The considered neutron energy interval - analogous to [9] - starts with $E_1 = 0$ eV and ends at $E_2 = 1$ eV for the reaction ^{139}La $(n,\gamma)^{140}$La as about 90% of the entire B value have been formed over this neutron energy interval [9]. Practically, mostly low-energy neutrons up to 1 eV contribute substantially to this reaction. In our experiment the corresponding cross section is $\sigma_{eff}(n,\gamma) = 7.2$ b

(see Table 8 in Ref. [9]). Using this analytical procedure one can calculate the experimental low-energy neutron fluences ($E < 1$ eV) for all the reactions under study. The results are given in Table 7 together with the experimental low-energy neutron-fluence $\Phi_n(E)_{exp}$ and some theoretical neutron fluences.

Table 7. Some theoretical and experimental neutron fluences on the outer mantle surface of the moderator, normalised to one incident proton.

System	n/p		$\Phi_n(E)_{theor}$ all energies		$\Phi_n(E)_{theor}$ low-energy (<1eV)		$\Phi_n(E)_{exp}$ low-energy (<1eV)
1.5 GeV p + Pb	25.1	(1)	18.6	(1)	5.9	(1)	11 ± 3
			17.5	(2)	3.8	(2)	
1.5 GeV p + U(Pb)	43	(1)	38.2	(1)	13	(1)	21 ± 5
3.7 GeV p + Pb	43	(1)	34.2	(1)	10.6	(1)	38 ± 6
	41	(2)	34.3	(2)	7.7	(2)	
3.7 GeV p + U(Pb)	79	(1)	67.9	(1)	25	(1)	65 ± 10
7.4 GeV p + Pb	61.5	(1)	50.5	(1)	17	(1)	45 ± 9
7.4 GeV p + U(Pb)	140	(1)	117	(1)	41	(1)	96 ± 20

(1) Calculated directly with the DCM-CEM code up to 10.4 MeV neutrons.

(2) Calculated directly with the LAHET code up to maximum energy neutrons.

n/p: Number of secondary neutrons emitted during the nuclear cascade calculation

    per incident proton.

$\Phi_n(E)_{theor}$: The total neutron fluence on the outer mantle surface calculated by theoretical models.

$\Phi_n(E)_{exp}$: The total experimental low-energy neutron fluence, determined with the La sensors (for details see the text and equations (6) and (7)).

The results from Table 7 are as follows:

1) Both theoretical models give very similar values for the total neutron fluences integrated over all neutron energies, although the amount of low-energy neutrons, as calculated by the two models, differs by up to 50%.

2) Despite the spread of low-energy neutron fluences calculated theoretically, all experimental low-energy neutron fluences based on La sensors are substantially larger than the theoretical fluences. These results, of course, reflect the results of Table 3 with the large values of $R(B)$ in the reaction ^{139}La $(n,\gamma)^{140}$La. Similar calculations can be done for other neutron sensors, giving rather similar, however less drastic results.

The results from Table 7 allow estimating the low-energy neutron fluence in an accelerator coupled "energy-amplifier" based on our experiments as follows:

- A 10 mA proton beam of 1.5 GeV on a Pb target system (Fig. 1) could have on the outer surface of the moderator a low-energy neutron fluence in the range of:

$$\Phi_{n,exp}(E)_{low-energy} = (2-4) \cdot 10^{14} \text{ n/s·cm}^2.$$

All technological aspects, such as heat production, radiation damage, etc. are neglected. Inside the moderator, the thermal fluences could be up to a factor 5 larger than on its surface, as will be shown experimentally later and as was shown in Ref. [9].

The observed transmutation rates B for ^{129}I and ^{237}Np allow estimating the transmutation capacity for a 10 mA and 1.5 GeV proton accelerator coupled to the Pb target (Fig.1) as follows:

- 1. Placed on the outer mantle of the moderator covering the Pb target and irradiated with 10 mA and 1.5 GeV protons for one month, 0.3% of ^{129}I could be transmuted into ^{130}Xe.

- 2. Placed on the outer mantle of the moderator covering the Pb target and irradiated with 10 mA and 1.5 GeV protons for one month, 6 % of ^{237}Np could be transmuted into ^{238}Np.

Again all technological aspects of this transmutation process, which are of course very complicated, had to be neglected.

Finally one can estimate the effective transmutation cross section $\sigma(n,\gamma)$ for ^{129}I and ^{237}Np using equation (6). We use values for the experimental low-energy neutron fluence as given in Table 4. One estimates for all the reactions:

$$\sigma(^{129}\text{I}(n,\gamma)^{130}\text{I}) = (8 \pm 4)\, b,$$

$$\sigma(^{237}\text{Np}(n,\gamma)^{238}\text{Np}) = (60 \pm 30)\, b.$$

These cross sections are lower than the known $\sigma(n,\gamma)$ cross section for ^{129}I (30 b) and ^{237}Np (180 b). (Note: the 30 b value for ^{129}I has been obtained from Ref. [21]). The reason for our lower cross sections could be the very hard neutron spectrum in our experiment, as compared to measurements in the pure thermal neutron fluences.
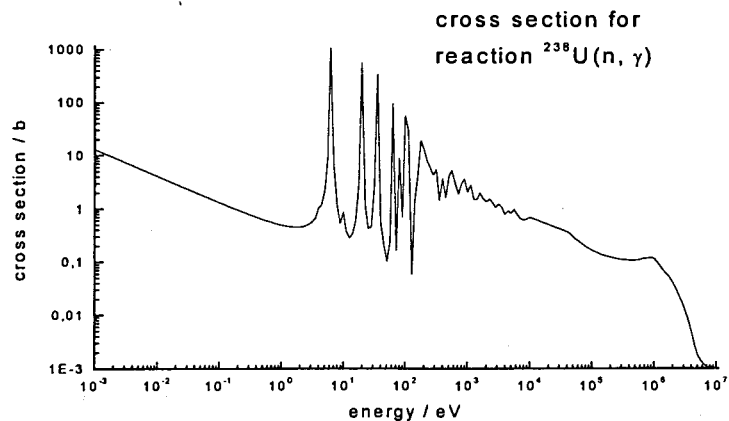
cross section for reaction $^{238}U(n, \gamma)$

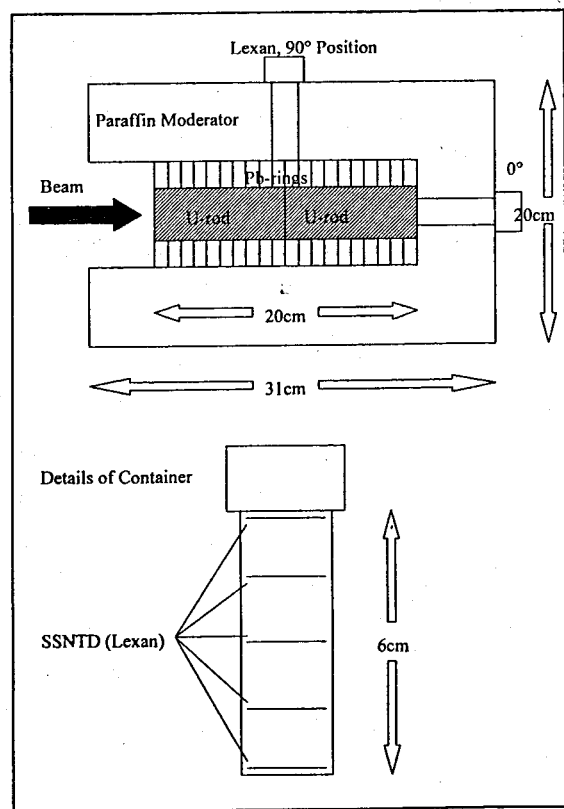Fig.12. Excitation function for the reaction $^{238}U(n, \gamma)^{239}U$

Fig.13. Lexan SSNTDs placed in a "container" positioned inside our experimental target setup

2.4. Supplementary experiments on secondary neutron fluences using solid state nuclear track detectors (SSNTD)

The radiochemical work was supplemented by some SSNTD studies. They provide further experimental details.

2.4.1. The determination of thermal and epithermal neutrons on top of the paraffin moderator [22]

An experiment was carried out with LR-115 SSNTDs to study the fluence of thermal and epithermal neutrons at all the three proton energies employed. Three targets were always placed on top of the moderator: one close to the beam entrance, one - in the centre and one - at the end of the moderator. The targets were exposed to a few beam pulses of the Synchrophasotron with a total fluence of approximately 10^{11} protons. In this case the proton beam fluence could not be checked independently with radiochemical sensors. The results for each experiment are given in Table 8 as an average of the three samples exposed. Comparing with the results in Table 7, one can find fewer neutrons at 1.5 and 3.7 GeV and the same number of neutrons at 7.4 GeV as compared to radiochemical sensors. Part of this discrepancy might be explained by impossibility to check independently the proton fluences and the beam profile in this experiment.

Table 8. Neutron fluences (per incident proton) as observed with LR-115 SSNTD on the outer mantle of the paraffin moderator

Exposure	$n_{thermal}$	$N_{epithermal}$
1.5 GeV p + Pb	4 ± 1	3 ± 1
1.5 GeV p + U/Pb	12 ± 2	8 ± 2
3.7 GeV p + Pb	19 ± 4	16 ± 4
7.4 GeV p + Pb	43 ± 11	34 ± 9
7.4 GeV p + U/Pb	105 ± 25	27 ± 6

2.4.2. Estimation of neutron fluences within the paraffin moderator using ^{235}U and ^{232}Th as target on Lexan [23]

In this study the major emphasis is placed on the determination of relative neutron fluences inside the paraffin moderator, as shown in Fig. 13. The SSNTDs were thin ^{235}U and ^{232}Th targets in contact with Lexan track detectors, the first target being sensitive to thermal neutrons, the second one to fast neutrons with $E > 2$ MeV. Two "containers" were placed at 90° and at 0° to the beam direction. Each plastic "container" had SSNTD sensors at 4, 5.5, 7, 8.5 and 10 cm from the beam axis. The results are shown in Table 9. As the irradiations were carried out only with a few bursts,

yielding approximately 10^{11} protons, the uncertainties in the absolute neutron number are large, as mentioned above. However, relative yields within one "container" are quite representative.

The results of Table 9 confirm the previous data, as given in Ref. [9], in more detail:

1. The effective fluence of thermal neutrons is in the centre of the paraffin moderator ($d = 7$ cm) is by a factor of 4 larger than in the outer mantle of the moderator ($d = 10$ cm).

2. This pattern of fluences is the same at all primary proton energies and independent of the metallic target (U or Pb).

3. One observes about the same pattern for thermal neutrons in the 0°-container as at 90°. However, the fluence of energetic neutrons ($E > 2$ MeV) increases considerably. This is to be expected from high-energy reactions.

Table 9. Effective ratio of neutrons to protons observed inside the paraffin moderator (Fig. 13); details will be presented elsewhere [23]

Reaction	distance d (cm) at 90°					distance d (cm) at 0°				
	4	5.5	7	8.5	10	4	5.5	7	8.5	10
1.5 GeV $p + $U										
^{235}U *	20	30	28	22	6	17	23	23	14	6
^{232}Th **	11	-	8	-	5	44	-	-	-	63
7.4 GeV $p + $U										
^{235}U *	103	166	206	127	45	-	-	-	-	-
^{232}Th **	27	-	181	-	17	-	-	-	-	-
7.4 GeV $p + $Pb										
^{235}U *	-	16	19	10	5	11	13	14	8	3
^{232}Th **	-	-	4	-	10	22	-	25	-	29

* Results for thermal neutrons, as measured with ^{235}U.

** Results for high-energy neutrons ($E > 2$ MeV), as measured with ^{232}Th.

The uncertainties are about 20%, without taking into account the uncertainties in the measurements of the proton fluences.

2.4.3. The distribution of thermal and epithermal neutrons on top of the paraffin moderator in the (7.4 GeV $p + $Pb) experiment [24]

· Two strips of LR-115- II B SSNTDs of length 31 cm and width of ~ 1 cm wide were placed on top of the paraffin moderator during the 7.4 GeV $p + $Pb irradiation. One of the strips was covered with a Cd foil. Thermal and epithermal neutrons were registered by the detector without Cd covers by means of ^{10}B (n,α) ^{7}Li reactions while the detector with Cd cover registered mainly the epithermal neutrons. The results are shown in Fig. 14. It is confirmed that the fluence of thermal neutrons even at this large proton energy (7.4 GeV)is well centred about 11 cm behind the entrance of the beam into the lead. Furthermore, the figure gives a more detailed picture how neutrons are distributed on the moderator surface, in particular it shows a hump in the middle of the distribution just above the lead target cylinder. At present it is not clear to us whether such behaviour has any dependence on the proton energy and the type of the target or not. The distribution of the epithermal neutrons is also shown in Fig. 14. Further details will be published [24].

2.4.4. The hardness of neutron spectra along the top of the paraffin moderator at 1.5 and 7.4 GeV irradiations [25]

Another technique has been employed to determine the "hardness" of the neutron spectra at a certain geometric position with the help of SSNTD. The details of the experiment will be published separately [25]. Fission cross sections are determined with a variety of actinide nuclides having a different threshold for (n,f)-reactions. Here we show the results for the ratio S with $S = \sigma_f(^{238}$U$) / \sigma_f(^{235}$U$)$ for all the four irradiations described earlier. Thin actinides are placed on SSNTD and irradiated on top of the moderator. The samples were etched to reveal the fission tracks. The track density on the surface of the SSNTD was determined using optical microscopes. The results are shown in Figs. 15 and 16. The ratio S is rather small close to the entrance of the beam into the metallic target ($d = 7$ cm), remains fairly constant over the main part of the moderator and increases sharply close to the downstream end of the moderator, indicating a drastic increase of high energy neutrons (> 2 MeV) inducing fission in ^{238}U. As we have placed the ^{129}I target close to the beam entrance and ^{237}Np targets more downstream, both target systems are exposed to different neutron spectra: ^{237}Np is exposed to a much harder spectrum than ^{129}I. However, as has been explained earlier, the uncertainties in the determination of (n,γ) cross sections are at present too large to allow further considerations.

2.4.5. The energetic part ($E > 10$ MeV) of the neutron fluence on the surface of the metallic target [26]

Thin slides of CR-39 (20 cm long, 1 cm wide and 1 mm thick) were placed along the axis of the metallic targets at the three energies under investigation. CR-39 is - after proper etching - sensitive to energetic hadrons of energies in the range of 10 MeV. The density of recoil protons is counted and their decrease along the axis is shown in Fig. 17. The track density decreases less steep
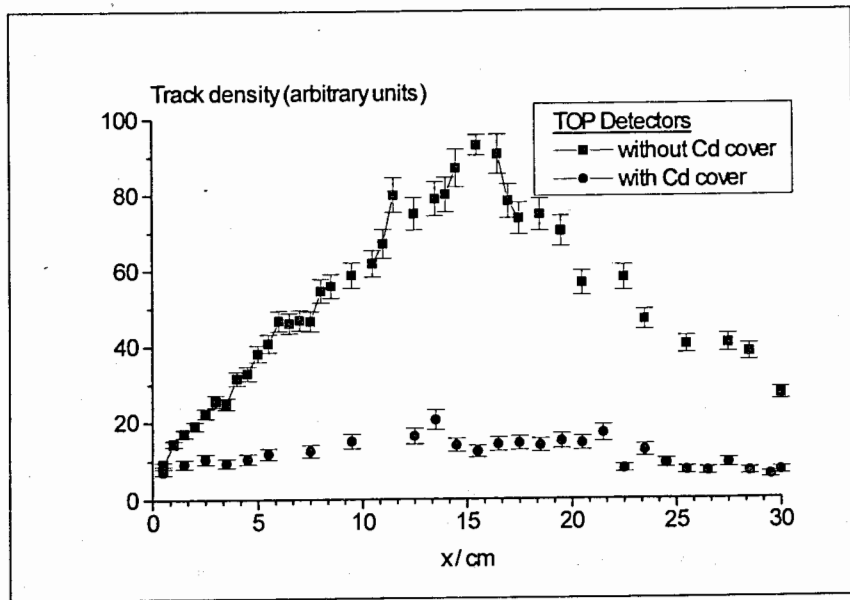
Fig.14. Thermal (without Cd cover) and epithermal (with Cd cover) neutrons detected on top of the moderator with LR-115- II B SSNTD [24] as observed in the reaction 7.4 GeV p + Pb
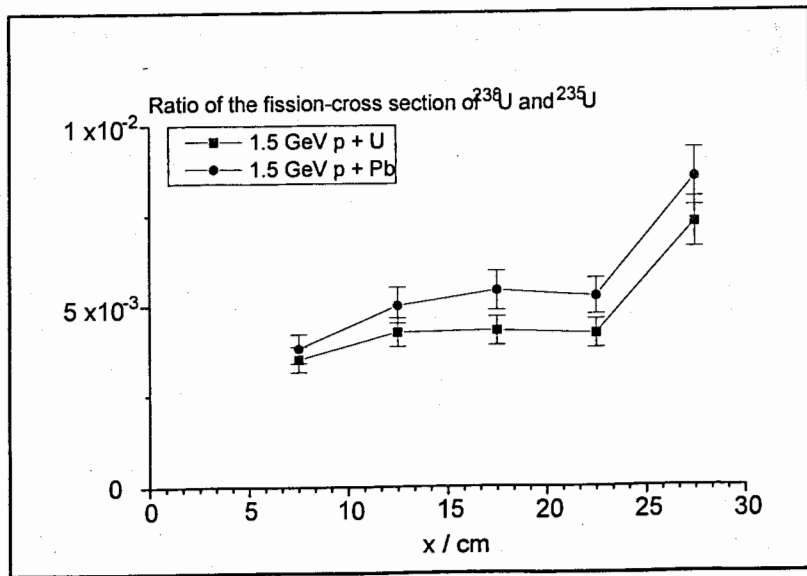

Fig.15. Ratio S of the cross-section for the fission of ^{238}U and ^{235}U on top of the moderator during the Pb- and U-targets [25] experiments with 1.5 GeV protons
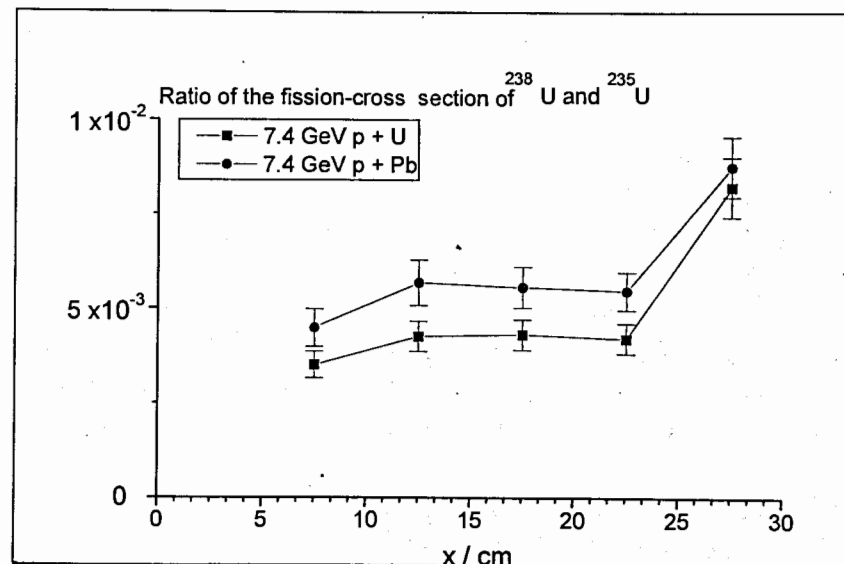

Fig.16. Ratio S of the cross-section for the fission of ^{238}U and ^{235}U on top of the moderator during the Pb- and U-targets [23] experiments with 7.4 GeV protons
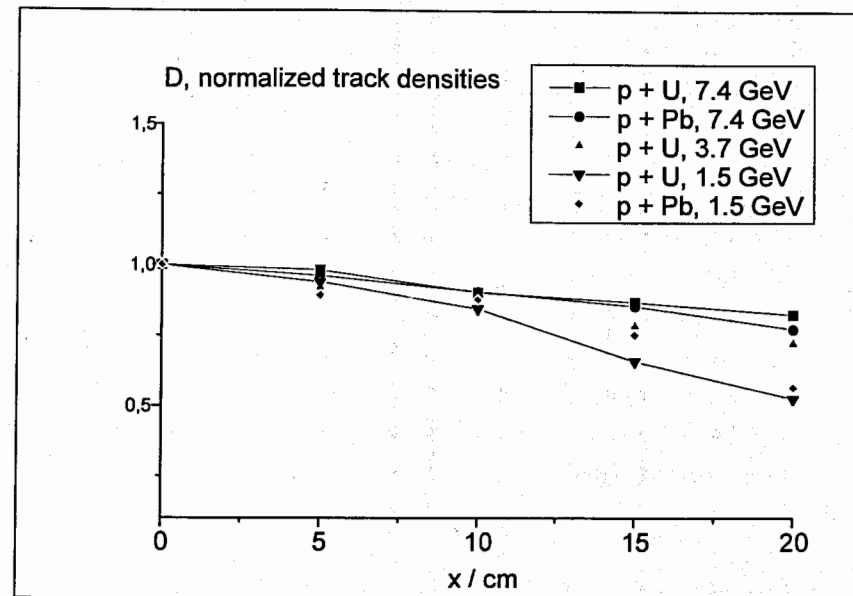

Fig.17. Normalized track densities in CR-39 detectors attached to the metallic surfaces of the 20cm long Pb or U(Pb) targets

the larger the incoming primary proton energy is. This effect has been observed in related experiments earlier [18].

2.4.6. The very energetic part ($E > 30$ MeV) of the neutron fluence on the surface of the metallic target [27]

Finally, it is also interesting to determine the secondary neutrons with $E > 30$ MeV. Such energetic particles can induce fission in gold. Consequently, a thin layer of gold with target thickness $T = 0.93 - 1.65$ mg/cm^2 was evaporated on the surface of a 1 cm^2 annealed mica plate and placed in the center of a 20 cm long metallic target between the metal and the paraffin moderator. After the exposure the mica was etched and the track density D was determined by optical observation. The results are shown in Table 10. Details will be published elsewhere [27].

Table 10. Track-density D, target thickness T (mg Au/cm^2) and normalized track density $D/\Phi \cdot T$, the total uncertainty is approximately 20%

Experiment	D, tracks / cm^2 *	T, mg Au/cm^2 **	$D/\Phi \cdot T$ ***
1.5 GeV p + Pb	5070	1.59	$2.2 \cdot 10^{-10}$
1.5 GeV p + U(Pb)	5340	1.46	$2.4 \cdot 10^{-10}$
3.7 GeV p + Pb	20900	0.93	$18 \cdot 10^{-10}$
3.7 GeV p + U(Pb)	33700	0.98	$28 \cdot 10^{-10}$
7.4 GeV p + Pb	22300	1.54	$15 \cdot 10^{-10}$
7.4 GeV p + U(Pb)	19100	1.65	$12 \cdot 10^{-10}$

*   Track density, uncertainty: 2%.

**   Target thickness, uncertainty: 5%.

*** The fluence Φ is taken from Table 1, uncertainty: (15-20)%.

Taking a fission cross section of 150 mb for high-energy neutrons, one can estimate a high-energy fluence ($E > 30$ MeV) of approximately 0.7 neutrons per 1.5 GeV p, 2.0 neutrons per 3.7 and 7.4 GeV p interacting with the Pb target. This is in approximate agreement with theoretical estimations (DCM-CEM gave about 1.6 neutrons at 1.5 GeV p + Pb, LAHET gave about 2.5 neutrons at 3.7 GeV p + Pb).

2.4.7. Beam profile measurements within the thick metal targets [28]

The beam profile has been measured by using a Lavsan-SSNTD in contact with a 8 cm in diameter Pb foil in contact with the front metal targets. A second detector was placed 10 cm, a third
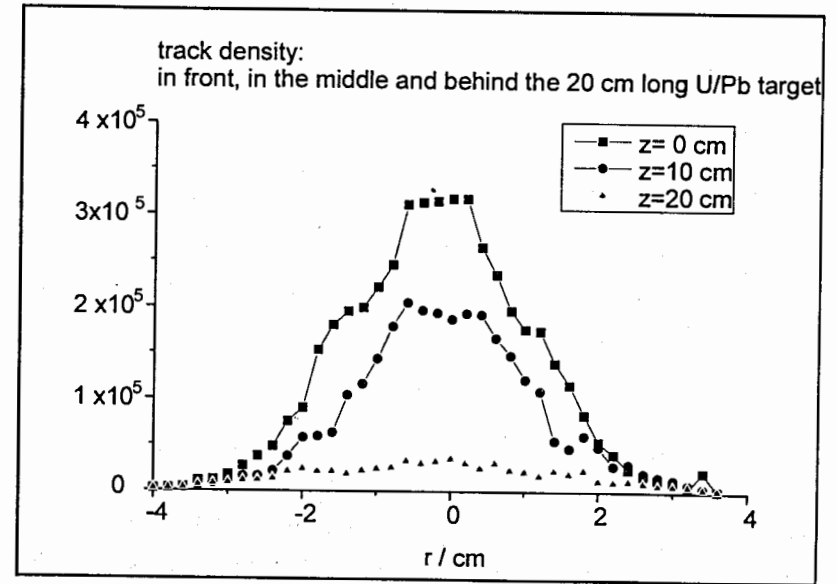

Fig.18. Beam profile of the Synchrophasotron for an extracted 1.5 GeV proton beam: in front of the target (x=0 cm), in the middle of the 20 cm long target (x=10 cm) and at the end of the target (x=20 cm) in a U(Pb) target, as measured with Lavsan SSNTD in contact with Pb

20 cm downstream. This system was exposed to the entire proton irradiation. Afterwards, the Lavsan foil was etched and the fission track density distribution along the 8 cm diameter was measured using an optical microscope. An example is shown in Fig. 18 for the 1.5 GeV proton irradiation. At 7.4 GeV proton energy the beam is focused better by a factor of 2. Another interesting feature of these measurements is the variation of track densities as a function of depth within the metal target. For 7.4 GeV protons, one can observe an increase in track densities within the first 10 cm of the targets, then a decrease. At 3.7 GeV one observes a decrease of $50 \pm 15\%$ between the first and the last detector, at 1.5 GeV an even stronger decrease as shown in Fig. 18. Details will be published elsewhere [28]. Similar behaviour of relativistic protons in thick targets have been determined in an independent experiment [18].

3. Conclusions

1. The transmutation rates for ^{129}I and ^{237}Np have been measured under specific geometric conditions. The absolute values of these transmutation rates are such that a 1 GeV proton

accelerator with 10 mA beam current can efficiently transmute ^{237}Np into shorter-lived ^{238}Np during one year. However, the transmutation of ^{129}I would be quite time consuming (many years) under the same conditions.

2. The neutron fluences on the surface of the paraffin moderator can be estimated experimentally and theoretically using computer codes (LAHET from Los Alamos, and DCM-CEM from Dubna). The experimentally determined thermal neutron fluences are substantially larger than the calculated ones. The precise reasons for this discrepancy are unknown. One may correlate this to an "enhanced nuclear cross section", observed in related experiments.

3. Experiments with solid state nuclear track detectors give valuable supplementary information about the nuclear interactions within the used target system.

References

1. Tolstov, K.D.: JINR preprint, 18-89-778, Dubna, Russia (1989)
2. Carminati, F. et al.: "An energy amplifier for cleaner and inexhaustible nuclear energy production driven by a particle beam accelerator", CERN preprint, CERN AT/93-47 (ET), Geneva, Switzerland (1993)
3. Bowman, C.D. et al.: "Nuclear energy generation and waste transmutation using an accelerator driven intense thermal neutron source", Nucl. Instr. and Meth. A 320 (1992) 336
4. Vassilkov, R.G. et al.: "Neutron yields from massive lead targets irradiated with light relativistic ions", Atomn. Energia 79 (1995) 257 (in Russian)
5. Abdullaev, I.G. et al.: "Neutron production in extended Cu-targets irradiated with relativistic ^{12}C-ions at Dubna, as studied with SSNTD and Nucl. Chemistry", Rad. Meas. 25 (1995) 219

6. Ochs, M. et al.: "SSNTD and radiochemical studies on the transmutation of nuclei using relativistic ions", Rad. Meas. 28 (1997), 255
7. Ochs, M.: PhD Thesis, FB Chemie, Kernchemie, Philipps-Universität, Marburg, ISBN 3-89703-050-0 (1997)
8. Krivopustov, M.I. et al.: "First experiments on transmutation studies on I-129 and Np-237 using relativistic protons of 3.7 GeV", JINR preprint E1-97-59, Dubna (1997); J. Radioanal. Nucl. Chem. Lett. 222 (1997) 267
9. Wan, J.-S. et al.: "Transmutation of radioactive waste with the help of relativistic heavy ions", JINR preprint, E1-97-349, Dubna (1997); Kerntechnik 63(1998)167
10. Andriamonje, S. et al.: "Experimental determination of the energy generated in nuclear cacades by a high energy beam", Phys. Lett. B 346 (1995) 697
11. Brandt, R. et al.: Nucl. Instr. Meth. 62 (1968) 110
12. Rudstam, G. et al.: Z. Naturforsch. 21a (1966) 1027
13. Silberberg, R. et al.: Astrophys. J. Suppl. 25 (1973) 35
14. Summerer, K. et al.: Phys. Rev. C 42 (6) (1990) 2546
15. Modolo, G.: Proc. Second Int. Conf. on Accelerator Driven Transmutation Technologies and Applications, Kalmar, Sweden, June 3 – 7, 1996, Editor H. Conde, Uppsala University, Vol. 1 (1997) 476
16. Hilscher, D. et al.: "Neutron multiplicity distributions for GeV proton induced spallation reactions on thin and thick targets of Pb and U", Proc. Int. Workshop on Nuclear Methods for Transmutation of Nuclear Waste: Problems, Perspectives, Cooperative Research, May 29 - 31, 1996, Dubna, Russia, 176; Phys. Rev. C 56 (1997) 1909
17. Rubbia, C., private communication: Seminar at CERN, Geneva, 06.12.1994.
18. Brandt, R. et al.: "Further evidence for enhanced nuclear cross-sections observed in 44 GeV carbon ion interactions with copper", JINR preprint E1-95-502, Dubna (1995); to be resubmitted to "Phys. Rev. C"
19. Zucker, P. et al.: "Spallation neutron production measurements", Proc. Second Int. Conf. on Accelerator Driven Transmutation Technologies and Applications, Kalmar, Sweden, June 3 - 7, 1996, Editor H. Conde, Uppsala University, Vol. 1 (1997) 527
20. Jain, P.L. et al.: "Abnormal behaviour of projectile fragments of a gold beam at relativistic energies", J. Phys. G, 24 (1998) 627
21. Reus, U., Westmeier, W.: Catalog of gamma rays from radioactive decay, Atomic Data and Nuclear Data Tables, Vol. 29, Nos. 1 and 2, July and September 1983

22. Zamani-Valassiadou, M., private communication, 04.06.1998, to be published

23. Debeauvais, M., private communication, 15.07.1998, to be published

24. Hashemi-Nezhad, S.R., private communication, 16.04.1998, to be published

25. Zhuk, I.V., private communication, 04.02.1998, to be published

26. Guo, S.L., private communication, 10.09.1998, to be published

27. Dwivedi, K.K., private communication, 16.04.1998, to be published

28. Perelygin, V.P., private communication, 20.06.1998, to be published